Composite Structures 348 (2024) 118511

Contents lists available at ScienceDirect

Composite Structures

journal homepage: www.elsevier.com/locate/compstruct

Mechanical characterisation and high temperature analysis of hyperelastic adhesives – Modelling and experimental validation

F.J. Simón-Portillo [a,*], E.A.S. Marques [b], M. Fabra-Rodriguez [a], L.F.M. da Silva [b], M. Sánchez-Lozano [a]

[a] Department of Mechanical and Energy Engineering, Miguel Hernandez University of Elche 03202, Spain
[b] Department of Mechanical Engineering, Faculty of Engineering, University of Porto, Porto 4200-465, Portugal

ARTICLE INFO

Keywords:
Temperature
FEM
Hyperelastic Models
Characterisation
Flexible Adhesives

ABSTRACT

Adhesive bonds are subject to multiple environmental conditions that can affect their mechanical performance during service. Therefore, it is important to evaluate the influence of temperature on adhesive strength, as it can impact joint safety and should be considered during the design phase. This study presents an analysis of the effect of high temperatures on the mechanical behaviour of joints made with highly elastic adhesives, specifically a polyurethane and a silicon-modified polymer. Shear and tensile tests were conducted at temperatures of 23, 50, and 80 °C using dumbbell specimens for tensile tests and single lap specimens (SLJ) for shear tests. The tests were performed with two different substrates, aluminium (Al) and glass fibre reinforced polyester panel (GRP), and with varying adhesive thicknesses. These tests aim to assess the impact of temperature conditions on the mechanical properties of the adhesive and the behaviour of the joints. The analysis of the experimental results reveals that the adhesive degrades when exposed to high temperatures, resulting in reduced strength and stiffness, and less linear behaviour.

Furthermore, this work involves the determination of a model able to reproduce the mechanical behaviour of hyperelastic adhesive at high temperatures, considering diverse constitutive modelling approaches. To achieve this, a testing protocol was conducted on basic uniaxial and planar specimens. The results indicate that the Ogden N=2 model is the most suitable for representing the non-linear behaviour of the hyperelastic adhesive at high temperatures. In contrast, the Mooney Rivlin model is more suitable to represent the material behaviour under ambient conditions. To conclude this work, the law has been satisfactorily validated by comparing the results of tests carried out on SLJ specimens with different adhesive thicknesses.

1. Introduction

Structural adhesive bonds have become a popular alternative to traditional mechanical joining techniques such as fastening and riveting. This is due to their numerous advantages, including lower weight, better fatigue behaviour, the ability to join dissimilar materials, and the potential to reduce manufacturing costs. As a result, adhesive bonds have replaced mechanical fasteners in various applications, including aerospace, automotive, and machinery. It is important to note that the use of structural composite materials, such as sandwich panels, and aluminium (Al) profiles, is on the rise in the manufacturing of industrial components. These materials are often assembled with highly flexible adhesives that are compatible with the high manufacturing tolerances and large deformations that they allow during use [1–4].

In practical applications, the joints are exposed to changes in humidity and temperature, which can have a negative impact on the joints [5]. In automotive applications, joints in close proximity to heat-producing components, such as the engine or exhaust manifold, frequently experience elevated temperatures compared to the surrounding environment. Furthermore, the performance of vehicle structural joints can be influenced by temperature fluctuations due to climatic conditions. According to some studies, these temperatures can reach as high as 80 °C [6,7].

The impact of temperature on adhesive bond strength is a crucial consideration during the design phase. The most significant factors affecting joint strength over a wide temperature range are adhesive

* Corresponding author.
E-mail addresses: f.simon@umh.es (F.J. Simón-Portillo), emarques@fe.up.pt (E.A.S. Marques), mfabra@umh.es (M. Fabra-Rodriguez), lucas@fe.up.pt (L.F.M. da Silva), msanchez@umh.es (M. Sánchez-Lozano).

https://doi.org/10.1016/j.compstruct.2024.118511
Received 4 March 2024; Received in revised form 25 June 2024; Accepted 18 August 2024
Available online 20 August 2024

shrinkage or expansion and changes in the adhesive mechanical properties. Studies that characterize the response of structural adhesives to temperature, mostly considering epoxy adhesives, generally show a decrease in strength as temperature increases [8–14].

To ensure that adhesives function properly, it is essential to study and optimize them. This can be done through finite element modelling (FEM) [15–18], but accurate and reliable results in joint simulation require precise material characterization activities. This research work focuses on highly flexible adhesives with non-linear elastic behaviour in the large strain range. This behaviour can be described employing hyperelastic material constitutive models [15,19–22], as these adhesives can reach high levels of deformation before failure.

This work firstly includes the mechanical characterization of hyperelastic adhesives subjected to high temperatures, employing tensile tests with dumbbell probes. The impact of high temperatures on single lap joints (SLJ) has also been studied, where different adhesive thicknesses (1 to 3 mm) and two types of substrates (aluminium (Al) and fibre-reinforced polyester (GRP)) were evaluated. These aspects are detailed in section 4.

The modelling phase consists on determining the behavioural law that best represents the material characteristics, based on test data from dumbbell (tensile) and planar (shear) specimens. The methodology previously developed by the researchers in this study has been applied to characterize the adhesive exposed to above ambient temperatures. Further details can be found in the paper, which characterizes the adhesive at room temperature [23]. On the other hand, the aim of this study is to demonstrate the general applicability of the characterization procedure at different temperatures.

After achieving a good fit of the hyperelastic model to the experimental data, the model can be used to simulate the behaviour of various joint configurations. To confirm the validity of the selected material model, computational modelling of SLJ joints subjected to high temperatures with different adhesive thicknesses was conducted. The numerical results were compared with the experimental results, which are detailed in section 5.

2. Experimental process/methodology

2.1. Materials

For this work, two materials commonly used as lightweight materials in the manufacture of vehicle bodies have been selected. Firstly, aluminium 6061 was selected, as it stands out for its high strength, remarkable stiffness-to-weight ratio, good formability and good corrosion resistance. [24]. The second material selected is GRP, which is a commonly used composite in commercial vehicle applications, which provides a good balance between cost, lightweight and mechanical performance. These materials are increasingly being considered as replacements for heavier materials, such as steel, due to the growing demand for weight reduction in the automotive industry. Table 1 provides details on the mechanical and physical properties of the materials used.

The study considered two commercial adhesives: SikaFlex 252, a one-component polyurethane adhesive manufactured by (Sika, Spain), and Henkel Teroson MS9360 (Henkel Adhesives, Germany) based on modified silane polymers. These adhesives are commonly used in the manufacture of vehicle bodies and the marine industry due to their ability to provide strong, flexible bonds with a low elastic modulus. Furthermore, they exhibit remarkable resistance to moisture and weathering [25]. Both adhesives cure by reaction with moisture.

Table 1
Mechanical and physical properties (Al and GRP) (Manufacturer properties).

	Aluminium (Al)	Fibre-reinforced polyester (GRP)
Youngs modulus (MPa)	68,900	2000
Tensile strength (MPa)	240	58
Density (g/cm^3)	2.7	1.3
Thermal conductivity (W/ (m K))	180	0.4

2.2. Thermomechanical analysis of adhesives

When studying bonded joints that will operate under wide temperature ranges, it is important to first determine the glass transition temperature (T_g) of the adhesive. Adhesives behave like a rigid, brittle material when tested below this critical temperature, while above the T_g the adhesive adopts a more elastic and rubbery nature.

The TA Instruments Q800 (EE.UU) Dynamic-Mechanical Analysis (DMA) instrument was used to measure the thermomechanical properties. The samples had a rectangular prismatic shape with 20 mm of length, 5 mm of width, and 2 mm of thickness. The experimental conditions consisted of a testing frequency of 1 Hz, a strain of 0.05 %, and a heating rate of 2 °C/min, in a temperature range of −90 °C to 100 °C. The obtained data facilitated the determination of the storage modulus (E') and loss modulus (E). The T_g was established from the most prominent peak in the loss modulus curve [26,27]. The Tg value was determined in accordance with the ISO 6721–11 standard.

T_g values of −59.1 °C and −80 °C were determined for SikaFlex 252 and Teroson MS 9360 adhesives, respectively. These temperatures are well below the usual working temperatures of the adhesive, indicating that these adhesives exhibit hyperelastic behaviour similar to that of rubber. Therefore, under the considered conditions, the behaviour of these adhesives can be modelled using hyperelastic models fitted from experimental data.

Furthermore, the dissipation factor (tan δ) was assessed. This factor is defined as the ratio of the loss modulus (E') to the storage modulus (E') and reflects the energy dissipation capacity of a material. It is represented as a dimensionless value, where a higher number indicates a higher proportion of non-elastic behaviour, and a lower number indicates a predominance of elastic behaviour. The analysis of adhesives revealed that the SikaFlex 252 adhesive reaches its maximum damping efficiency at a temperature of −48.1 °C, whereas for the Teroson MS 9360 adhesive, this is achieved at −54.1 °C.

2.3. Test conditions

Three representative thermal levels have been chosen for this study: 23, 50, and 80 °C. These temperatures were selected because certain vehicle components can reach them during operation, representing the most extreme cases during operation [28,29]. An Instron Model 3367 universal testing machine (Norwood, MA, USA), equipped with a 30 kN load cell, was used to conduct the tests. An environmental chamber, integrated within the testing machine, was used to achieve the required temperatures during the tests (Fig. 1a). Four joints were tested to failure for each temperature and specimen configuration, allowing to demonstrate a high degree of repeatability in all cases. To ensure an uniform temperature inside the chamber, the specimen was held at the desired test temperature for 30 min before the first test was started. Each subsequent test was started 20 min after inserting the specimen, allowing to ensure even temperature distribution throughout the chamber. A thermal study was conducted through simulation to verify thermal uniformity in the SLJ joint. The boundary conditions are convective heat transfer from the oven air at a temperature of 50 °C, applied to the external surfaces of the specimen at initial ambient temperature. The results indicate that the temperature is uniform throughout the specimen volume after 15 min, as shown in the cross-section of Fig. 1b.

2.4. Fit tests of the hyperelastic model

To obtain the constants of the 1st and 2nd order hyperelastic models, stress–strain curves in two different loading configurations are required [30,31]. Uniaxial tensile test with dumbbell specimens and planar test,

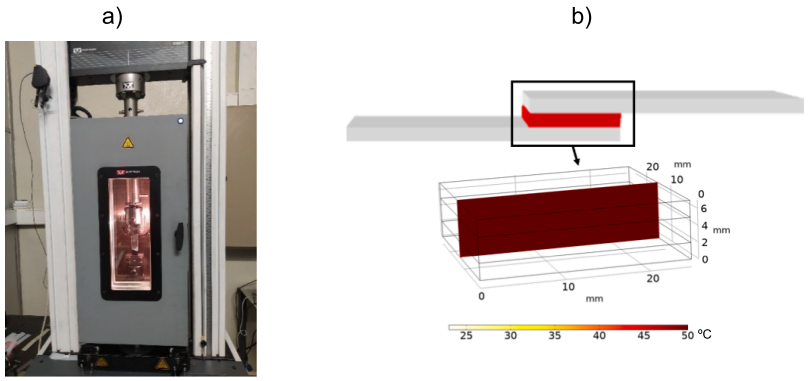

Fig. 1. a) test machine and climatic chamber; b) fem thermal analysis.

also known as "pure shear", were chosen. Furthermore, it is highly recommended to include the latter test in the characterisation of hyperelastic materials in order to take into account the shear behaviour of the material [32].

The study employed planar specimens made of thin adhesive sheets that were subjected to tensile stress. There is no standard for the dimensions of the planar specimen. Specimens with dimensions of 150 mm width by 90 mm total length, with an effective length of 50 mm and 3 mm thickness are used (Fig. 2). These dimensions were selected in a previous study by the authors of the present work [23]. Each specimen underwent a curing process in a controlled room at 23 ± 3 °C and 50 ± 5 % humidity, following the adhesive manufacturer's instructions. Periodic measurements of the hardness of the adhesive sheets were conducted using a Durotech hardness tester, model M202 (UK), to ensure proper completion of the curing process. The measurements remained constant (at 50 Shore A) from day 15 onwards, indicating complete curing of the adhesive.

A visual inspection was conducted to identify any internal defects in the adhesive sheets before removing the different specimen.

The clamps utilized for the planar test consisted of 17 mm thick birch plywood sheets and incorporated two steel plates to evenly distribute the pressure generated by the connecting bolts. To prevent adhesive slippage during the test, double-sided tape was placed between the wood and adhesive sheet. For further assembly details, please refer to the documentation [23].

Tests on the planar specimens were carried out at a controlled displacement rate of 150 mm/min [23]. Deformation was obtained by digital image correlation (DIC) [33,34] from images taken with a Nikon D5300 camera (Japan). The images were processed using the Tracker software (Fig. 3) [35]. This technique also allows the detection of debonding or slippage of the adhesive relative to the clamps.

Uniaxial tensile tests were carried out on dumbbell specimens, with dimensions corresponding to those defined in ISO 37:2005. The dumbbell specimens were obtained using a die-cutting machine, cut from a 3 mm thick adhesive sheet, previously cured and tested by the method described above. The dumbbell specimens were tested using the same equipment previously used for the planar specimens, except for the grips, which were adapted to the dimensions of the new specimens. A test speed of 200 mm/min was set for the dumbbell specimen, as defined in the standard. Strain data were also obtained using the DIC technique.

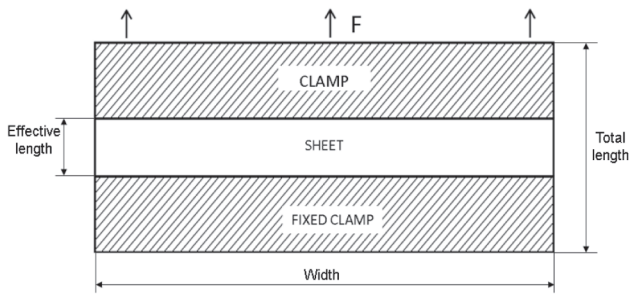

Fig. 2. Planar shear test geometry.

2.5. Adjustment of hyperelastic models

For the comparison between the different applicable models and the estimation of the corresponding hyperelastic constants, the Abaqus finite element software has been used. The program is used as an optimisation tool, taking the nominal stress and nominal strain curves from simple specimens that have been tested (dumbbell −planar). It estimates the constants of different possible models using the least squares method, based on the curves.

The input data required by the program includes the nominal stress-nominal strain curves, from which the program estimates the constants of the different possible models by means of least squares.

The material models considered were Neo-Hookean, Mooney-Rivlin (polynomial N=1) and Ogden (N=1, N=2 y N=3) [30,36,37]. It should be noted that in this case, the compressibility constants are zero for each of the models, as the material is assumed to be incompressible.

To determine the most suitable hyperelastic model for replicating the mechanical behaviour of the planar and uniaxial tests, the simulated curves of various models were compared with the experimental stress–strain curves. The validity of the mechanical behaviour of finite element (FE) models was examined using the correlation and analysis (CORA) method [38]. The results are detailed in section 4.

2.6. Application and validation of hyperelastic models with SLJ specimens

Four types of specimens were manufactured using different substrates (Al-GRP) and two adhesive thicknesses (1 and 3 mm). This study analysed the impact of high temperatures on various bonding configurations by testing different adhesive thicknesses and bonding materials. The fabrication of SLJ specimens is commonly described by ASTM D1002 and ISO 9664 standards. The specimens are composed of two substrates, each measuring 100 mm in length, 25 mm of width, and 3 mm of thickness, which are bonded together using an adhesive. The overlap length is 25 mm, and the adhesive layer thicknesses are 3 mm and 1 mm, as shown in Fig. 4a. All specimens were prepared in a stable and clean environment. The adhesive surfaces were degreased with acetone, and a primer, SikaPrimer 206, was applied to the substrates following the manufacturer's instructions. Finally, one hour after applying the primer, the adhesive was applied to the substrate. The thickness of the adhesive was accurately adjusted using specific tooling, with a tolerance of 0.1 mm. The specimens were then cured in a controlled room at 23 ± 3 °C and 50 ± 5 % humidity for 15 days [23].

The steel plates are placed in the clamps of the testing machine and a

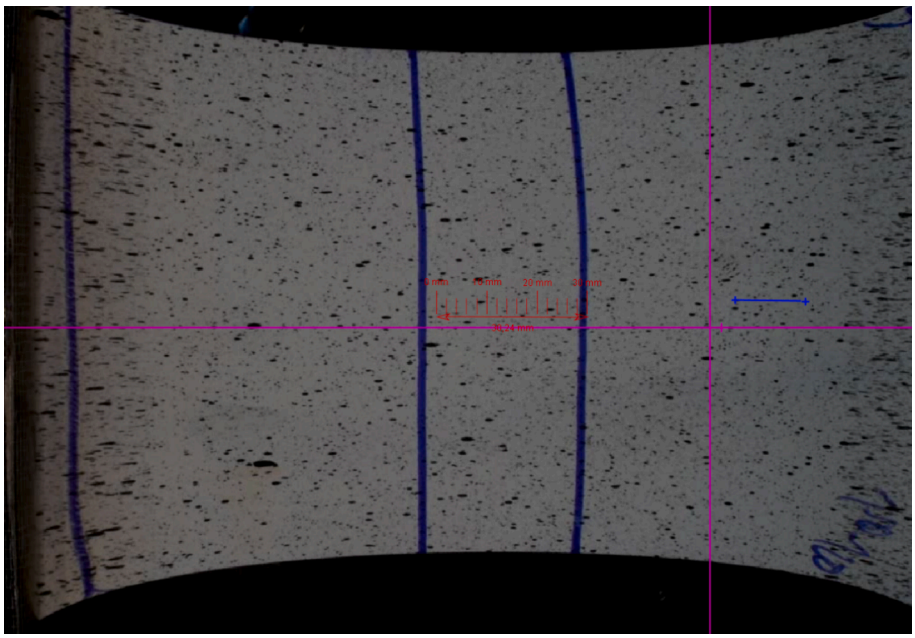

Fig. 3. Measurement of planar specimen deformation (Tracker).

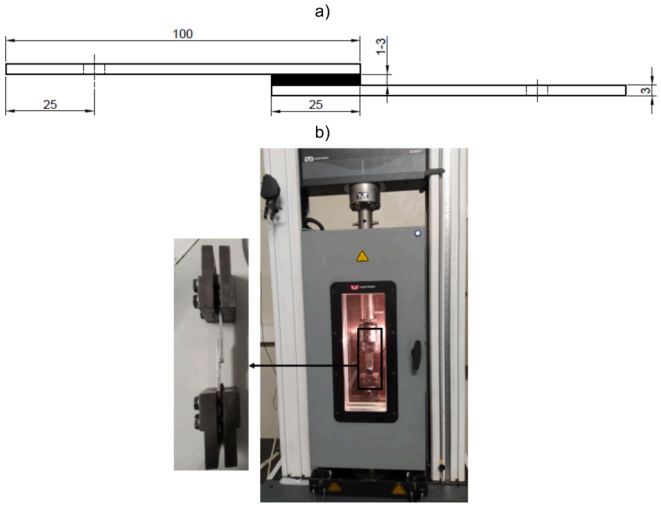

Fig. 4. a) slj specimen geometry (dimensions in mm); b) test equipment for slj specimen clamps.

displacement is applied to the moving clamp at a speed of 10 mm/min [12]. During the test, the clamp displacement and the force measured by the load cell are recorded. Due to the dimensions of the specimens and the configuration of the claws, only shear stresses are generated. This prevents uncontrolled deformations in the adhesive (see Fig. 5b).

To validate the model, SLJ specimens with adhesive thicknesses of 1–3 mm were simulated using FEM in Abaqus. The results of the numerical hyperelastic models that best fit the experimental results were compared and used the fitted constants of the combination of dumbbell and planar specimens. After conducting a mesh convergence study, element sizes of 1.5 mm for the aluminium plates and 0.2 mm for the adhesive in the SLJ specimen models were established. The convergence analysis is conducted by comparing the force value obtained for the 50 % displacement in the SLJ test of the strain to failure. The element types used in this study were hexahedral quadratic with reduced integration (C3D8RH). The boundary conditions were defined as shown in Fig. 5a. Movement at the left end of the specimen is fully restricted, while a displacement (u_x) is applied to the right end to reproduce the test conditions.

3. Experimental results and discussion

3.1. Temperature's influence on adhesive tensile behaviour

Fig. 6 shows the stress–strain curves for SikaFlex 252 adhesive at varying temperatures, as obtained from the dumbbell test. The results indicate that as temperature increases, both the deformation resistance and stiffness of the adhesive gradually decrease. At 50 °C, the failure strength of the adhesive decreases by 44 % compared to the test at 23 °C, and by 59 % at 80 °C.

Fig. 7 shows the stress–strain curves for Teroson MS 9360 adhesive obtained at different temperatures. It can be seen that, with the

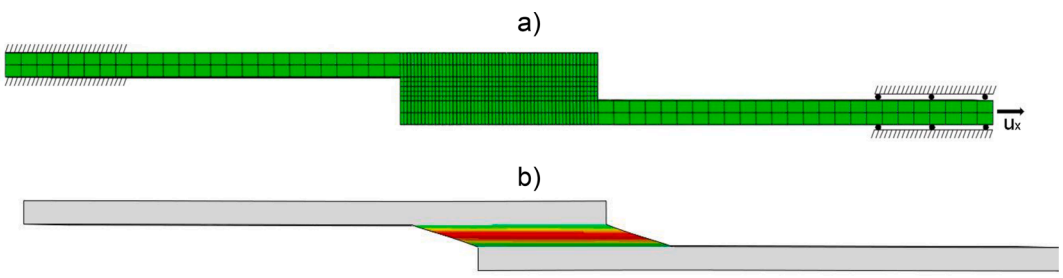

Fig. 5. a) boundary conditions slj; b) fem simulation slj.

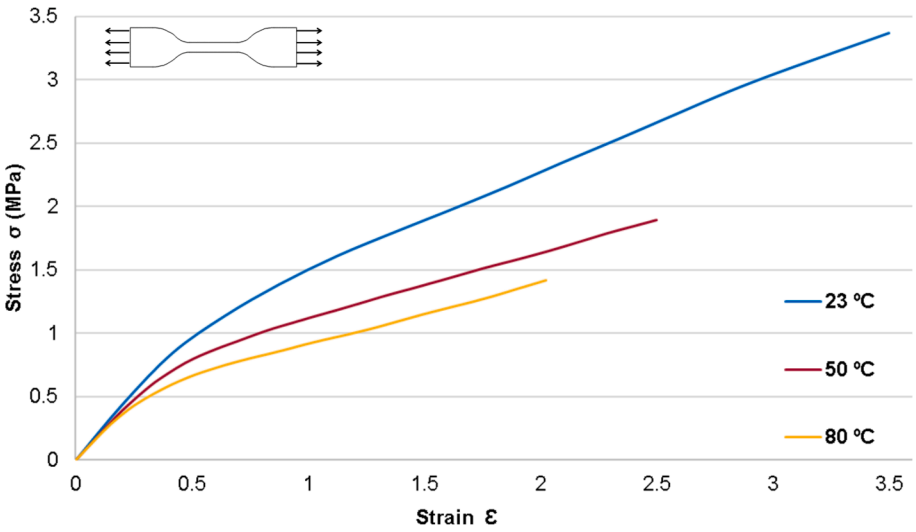

Fig. 6. Representative test of SikaFlex 252 adhesive at different temperatures (Dumbbell).

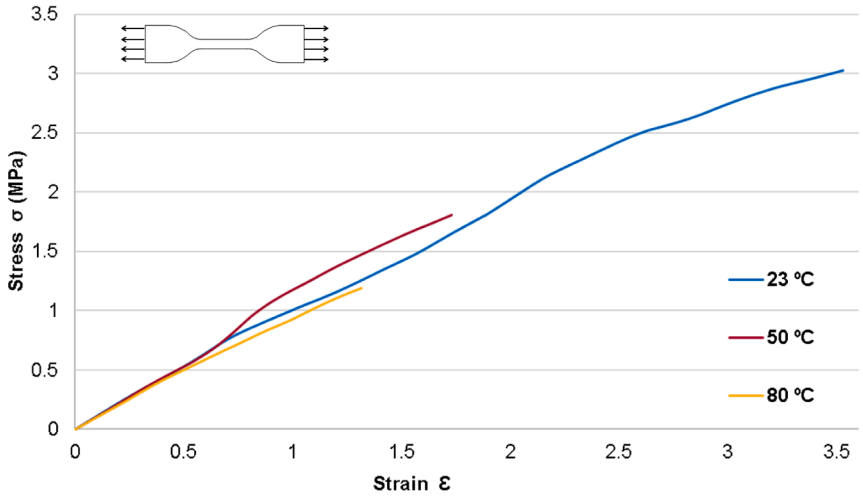

Fig. 7. Representative test of Teroson MS 9360 adhesive at different temperatures (Dumbbell).

increasing temperature, changes in both the failure load and the failure strain are observed. Compared to the results obtained at 23 °C, the failure load of the adhesive decreased by 43 %, at 50 °C and 60 % at 80 °C. The stiffness of the adhesive, however, remains largely unaffected.

Table 2 presents data on the maximum stress, maximum load, and maximum elongation of SikaFlex 252 and Teroson MS 9360 adhesives at different temperatures. The values are the average of four tests performed under the same conditions, with half of the maximum deviation shown within brackets. It is important to note that the evolution of failure load with temperature is similar for both adhesives. At 23 °C, both adhesives exhibit similar deformation capacity. However, the maximum elongation is noticeably influenced by high temperatures, with a more pronounced effect observed in the case of the Teroson MS 9360 adhesive.

For the statistical analysis, the T-Student distribution was used, establishing a 90 % confidence interval. All 4 results for each type of test are within the calculated confidence intervals.

3.2. *Effect of high temperatures on the shear behaviour of adhesives*

To proceed with the analysis of the impact of high temperatures on both adhesives, Fig. 8 displays the results obtained from tests on SLJ

Table 2
Mechanical properties of SikaFlex 252 and Teroson MS 9360 adhesive.

	SikaFlex 252			Teroson MS 9360		
	Max. Stress (MPa)	Max. Load (N)	Max. Strain (%)	Max. Stress (MPa)	Max. Load (N)	Max. Strain (%)
23 °C	3.3 (±0.1)	68 (±4)	350 (±5)	3.0 (±0.2)	61 (±5)	357 (±4)
50 °C	1.8 (±0.1)	38 (±3)	240 (±3)	1.7 (±0.1)	36 (±3)	173 (±5)
80 °C	1.4 (±0.1)	28 (±3)	199 (±6)	1.3 (±0.2)	24 (±2)	134 (±7)

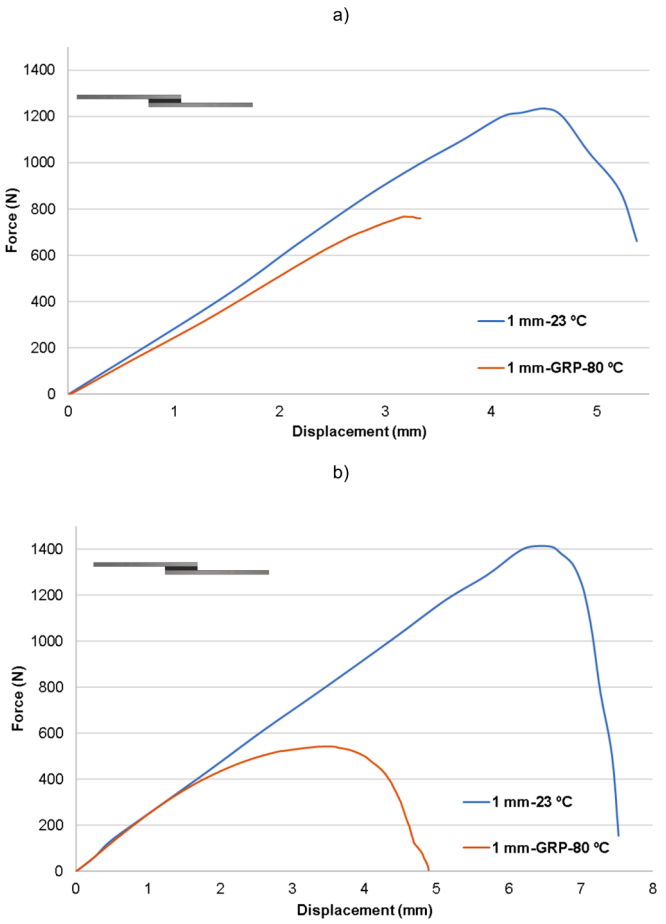

Fig. 8. a) experimental results slj (teroson ms 9360); b) experimental results slj (sikaflex 252).

specimens. These specimens are made of GRP with a 1 mm thick adhesive and were subjected to a temperature of 80 °C.

When analysing Fig. 8a, it is evident that the specimens produced using Teroson MS 9360 adhesive undergo a reduction in joint stiffness when exposed to 80 °C, until they reach deformations of 3 mm, at which point sudden rupture occurs. In contrast, Fig. 8b displays the outcomes of the experiments conducted with SikaFlex 252 adhesive, where a comparable behaviour of both joints is observed up to deformations of 2 mm. At 80 °C the joint exhibits increased ductility after 2 mm of deformation, until it ultimately reaches its breaking point.

3.3. *Effect of temperature on SLJ joints with different adhesives (Al and GRP)*

Fig. 9 shows the force–displacement curves obtained at different temperatures for SLJ joints made with different Al and GRP adhesives, using SikaFlex 252 adhesive with 1 mm of thickness.

It is evident that there is a degradation in performance at high temperatures, with joints made of Al being more significantly affected than GRP. This is due to the occurrence of adhesive failure. Furthermore, elevated temperatures have a detrimental impact on the surface treatment applied to aluminium and on the adhesive strength of the adhesive-aluminium interface. In the case of the joint exposed to 50 °C, there is a partial failure of the adhesive, as shown in Fig. 10b. The joint subjected to 80 °C experiences a drastic decrease in maximum load due to complete adhesive failure. Cohesive failure was observed in all cases for the GRP specimens, regardless of the adhesive thickness (1 mm or 3 mm), shown in Fig. 10a.

Fig. 11 shows the force–displacement curves obtained at different temperatures, using the same specimen configurations as in the previous case, but now with an adhesive thickness of 3 mm. Again, a decrease in bond performance is evident as the temperature increases. A reduction in stiffness is observed in all the tests of the joints made of aluminium for both temperatures, with partial adhesive failure occurring in the joints exposed at 50 °C. As for the joint exposed to 80 °C, a marked decrease in maximum load occurs, due to a total adhesive failure in all tests. It should be noted that the stiffness of all the specimens tested with an adhesive thickness of 3 mm shows a greater similarity between them compared to the specimens tested with a thickness of 1 mm.

Table 3 presents the failure loads of the SLJ joints for various temperatures and specimen configurations. The values displayed are the average of four tests conducted under identical conditions, with half of the maximum deviation shown in brackets. The results for the two adhesive thicknesses indicate that, within this specific range, there is no significant impact in the failure load. However, the failure load is always lower for the 3 mm adhesive layer thickness.

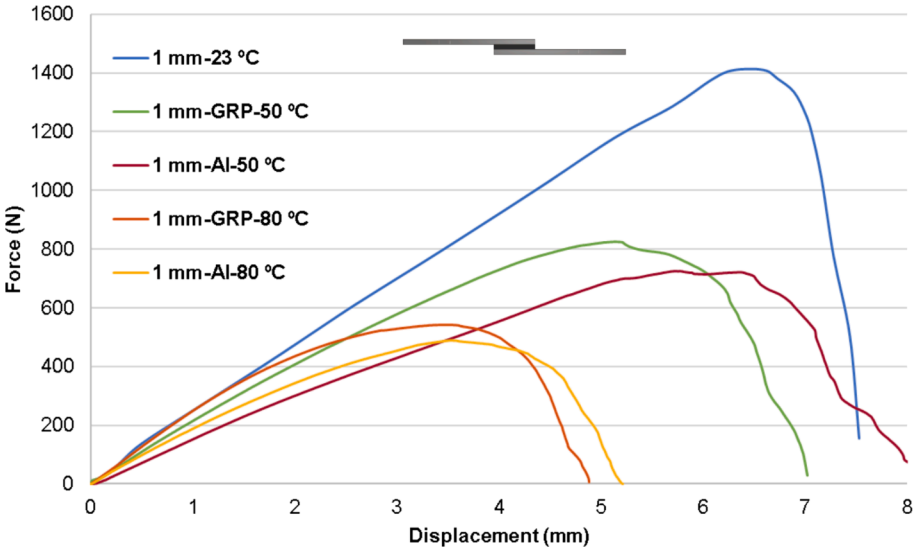

Fig. 9. Experimental results SLJ-1 mm of Al and GRP (SikaFlex 252).

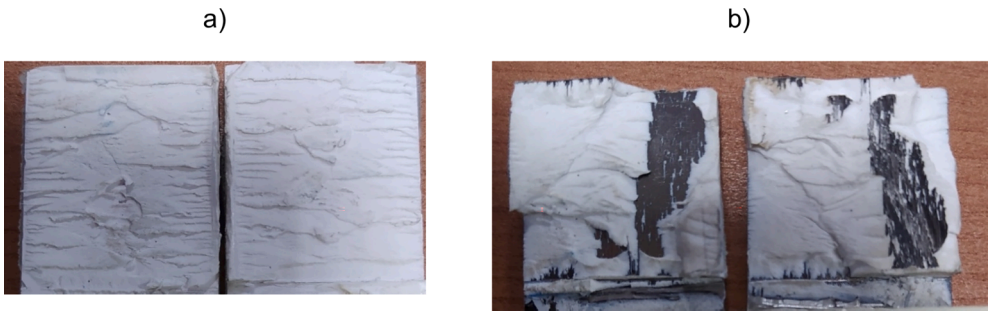

Fig. 10. Fracture surface of specimens tested. a) GRP (b) Al (SikaFlex 252).

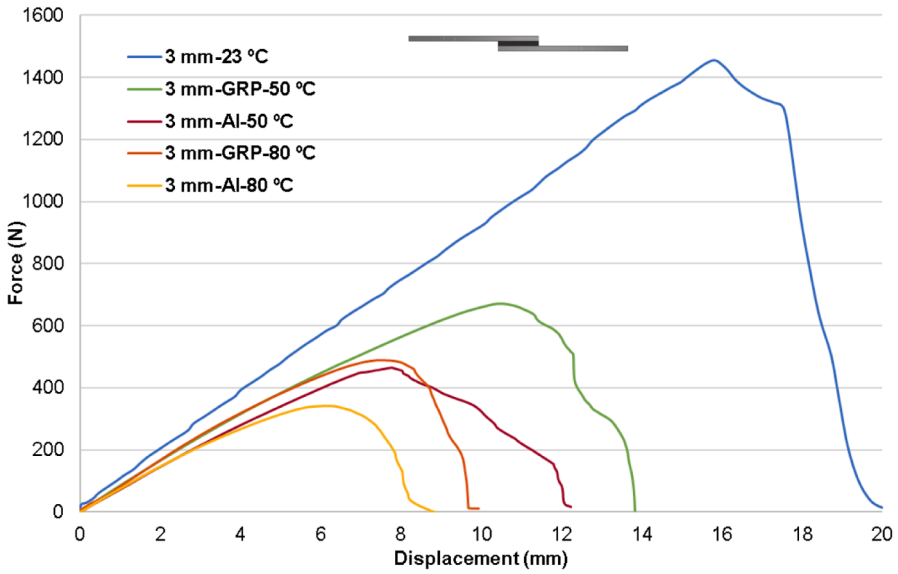

Fig. 11. Experimental results SLJ-3 mm of Al and GRP (SikaFlex 252).

Table 3
Failure loads of SLJ-1 mm and SLJ-3 mm (N).

	SLJ-1 mm			SLJ-3 mm		
	23 °C	50 °C	80 °C	23 °C	50 °C	80 °C
GRP	1400 (±10)	820 (±10)	500 (±10)	1450 (±10)	650 (±10)	450 (±10)
Al	1400 (±10)	700 (±10)	450 (±10)	1450 (±10)	430 (±10)	350 (±10)

4. Fitting and validation of hyperelastic models

4.1. Fitting of hyperelastic models

Figs. 12 and 13 present a comparison between the experimental results of the SikaFlex 252 adhesive at 50 °C and the different models considered. Analysing the plots, it becomes evident that the Ogden N=2 and N=3 models provide the best fit for the experimental results, both in the uniaxial and planar tests. However, it is not possible to visually determine which of the two models has the better fit.

Table 4 shows an evaluation of the curves with the CORA index to provide a quantitative comparison. The results indicate that the hyperelastic model that best reproduces the planar test is the Ogden model with N=2 (ratio = 0.929), followed by the Ogden with N=3 (ratio = 0.916). For the dumbbell test, the CORA evaluation shows that the best agreement with the experimental results is achieved with the Ogden N=3 model (ratio = 0.850), followed by the Ogden N=2 (ratio = 0.846). Despite these results, it is not possible to conclusively determine which model is the most appropriate. Therefore, the validation in the following section was carried out using the constants estimated for each model (Table 5-6).

On the other hand, the Ogden N=1 and Neo-Hookean models are those that present the greatest discrepancy with respect to the experimental curves, overestimating the stiffness in the uniaxial test and underestimating it in the planar test.

4.2. SLJ model validation

To determine which of the Ogden N=2 and N=3 models was more accurate, SLJ specimens with adhesive thicknesses of 1–3 mm were simulated at a temperature of 50 °C.

Fig. 14 shows the comparison between the results obtained with the Ogden models N=2 and N=3, with data obtained from the test corresponding to the SLJ joint manufactured with GRP adhesive (cohesive failure) and 1 mm of adhesive thickness. The Ogden model with N=2 shows a more acceptable correlation than that with the constants adjusted for the Ogden model N=3.

A closer comparison between the performance of the Ogden N=2 model and the experimental results (SLJ-1 mm) is depicted in Fig. 14. Here, the slope of both the experimental and numerical curves is strikingly similar up to 3 mm of deformation. However, beyond this point, the simulation exhibits a decrease in stiffness.

Fig. 15 compares the Ogden N=2 and N=3 simulations with the test data for the SLJ joints manufactured with GRP adhesive (cohesive failure) and 3 mm of adhesive thickness. The Ogden N=2 model shows the

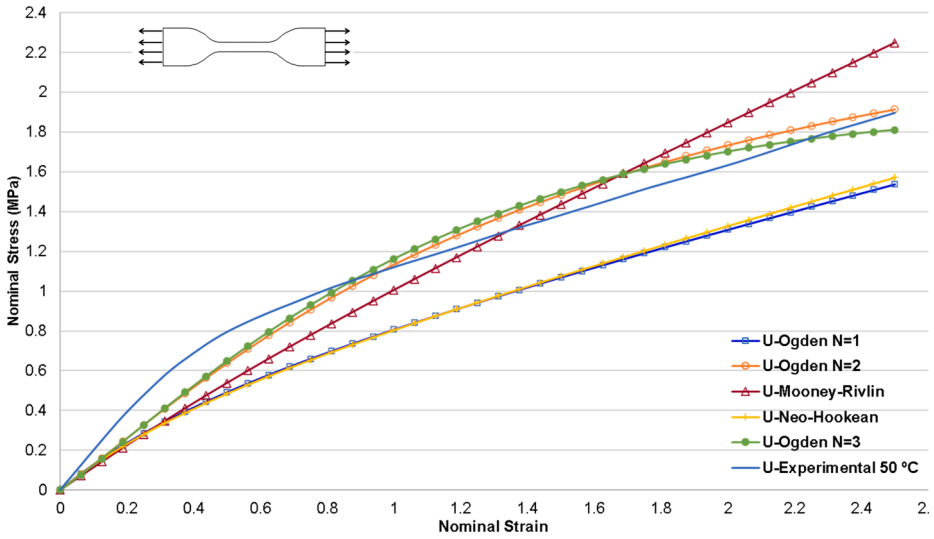

Fig. 12. Uniaxial test results for the considered models (SikaFlex 252).

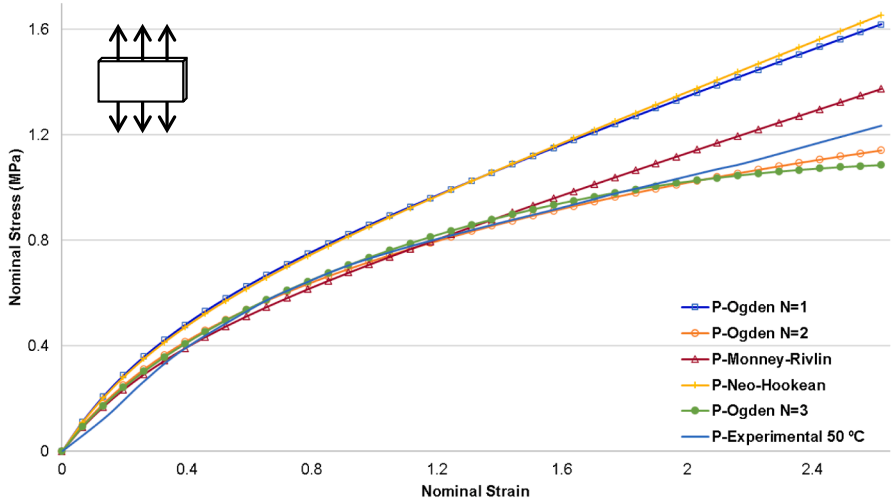

Fig. 13. Planar shear test results for the considered models (SikaFlex 252).

Table 4
CORA rating for different hyperelastic models fitted with 150 x 90 x 3 mm specimen planar test and uniaxial test with dumbbell specimen.

Model	R-Planar	R-Uniaxial
Ogden N=1	0.612	0.564
Ogden N=2	**0.929**	0.846
Ogden N=3	0.916	**0.850**
Mooney Rivlin	0.850	0.739
Neo Hookean	0.616	0.567

highest correlation in this configuration.

When comparing the Ogden N=2 simulation with the SLJ-3 mm experimental results, the curve obtained with the model accurately correlates with the experimental data up to deformations of 7 mm. Additionally, a decrease in stiffness is observed from this point onwards.

The results lead to the conclusion that the most accurate way to characterise the SikaFlex 252 adhesive under 50 °C conditions is by using the Ogden N=2 model.

Table 5
Adjusted constants for Ogden N=2.

N	μ	α	D_1
1	24.0656	0.279276	0
2	−23.6559	−0.139683	0

5. Conclusions

The experimental study shows that the strength of the adhesives under analysis decreases with increasing temperature, more significantly for the Teroson MS 9360 adhesive.

The polyurethane-based adhesive (Sikaflex 252) exhibits a progressive decrease in stiffness with temperature, with a more non-linear behaviour. In contrast, increasing temperature does not appear to affect the stiffness of the silane-modified polymer-based adhesive (Teroson MS 9360).

According to these results, modified silane-based adhesives would be more suitable for applications where it is important to maintain a constant level of stiffness regardless of temperature. But where it is

Table 6
Adjusted constants for Ogden N=3.

N	μ	α	D_1
1	183.196736	0.792642393	0
2	−80.6306379	0.931503049	0
3	−102.172637	0.650190003	0

considered more important that the breaking strength is less affected by temperature, polyurethane-based adhesives would be more appropriate. However, further testing with both types of adhesive would be necessary before these conclusions can be generalised.

An analysis of the response of the SLJs shows a decrease in bonding performance at high temperatures, mainly caused by the reduction in the ultimate strength of the adhesive. However, joints using aluminium as a substrate have shown even lower strength compared to those made of GRP due to adhesive failure. Additionally, temperature negatively affects the surface treatment applied to the aluminium and the adhesive strength of the adhesive-aluminium interface.

On the other hand, the model that best represents the behaviour of the polyurethane-based adhesive at different temperatures was determined. The material's behaviour at room temperature was found to be well represented by a Mooney Rivlin model. But the Ogden model with N=2 shown as the most effective in reproducing the adhesive's behaviour at 50 °C, mainly due to the deviation from linearity found at high temperature.

In light of these results, this work serves as further validation for the methodology used to characterise high flexibility adhesives, which was previously developed by the research group.

Finally, an extension of this study to other types of hyperelastic adhesives and temperatures is suggested. However, since changes in temperature can significantly impact the linearity of the mechanical

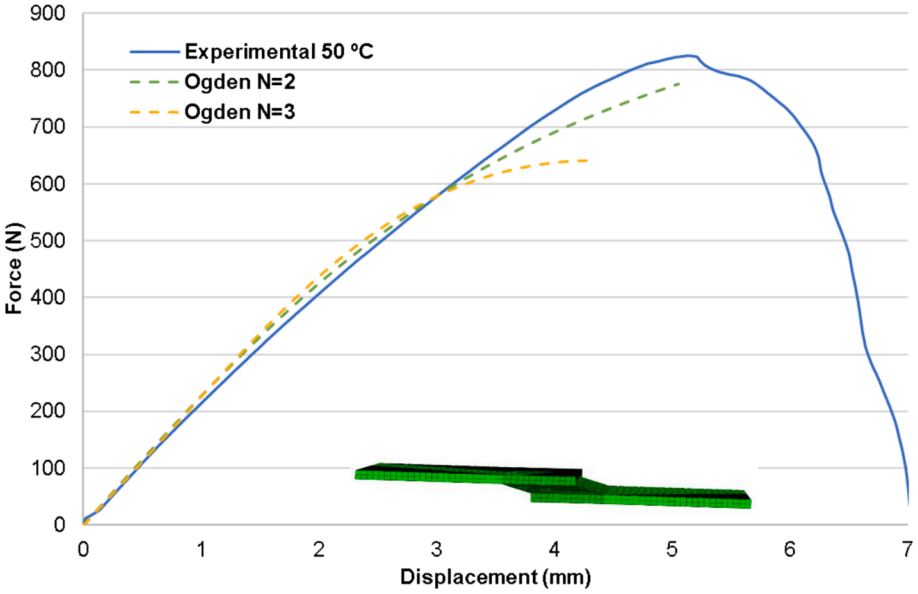

Fig. 14. Experimental and computational results for SLJ-1 mm. Comparison between the different models (SikaFlex 252).

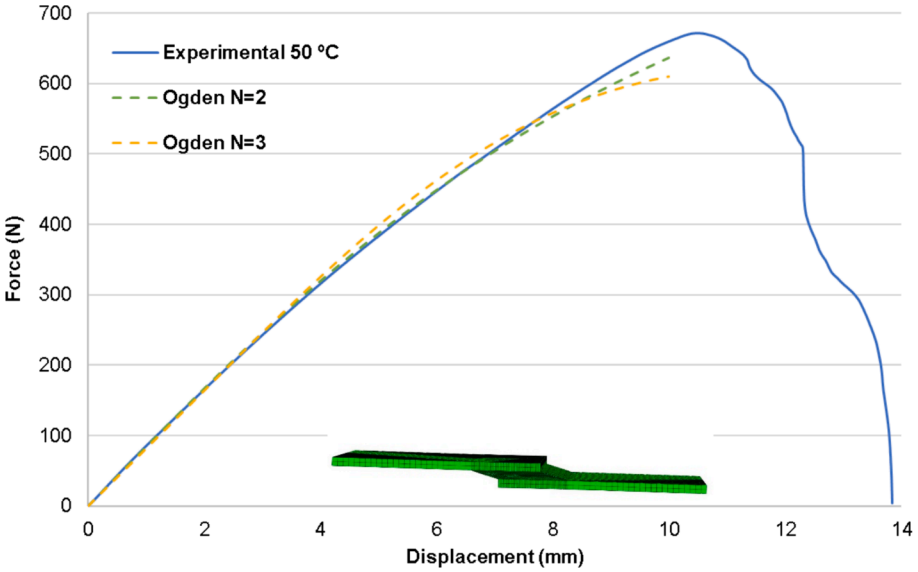

Fig. 15. Experimental and computational results for SLJ-3 mm. Comparison between the different models (SikaFlex 252).

behaviour of the adhesive it is also necessary to further explore the use of different models and behavioural laws to represent adhesive behaviour in large temperature ranges.

CRediT authorship contribution statement

F.J. Simón-Portillo: Writing – original draft, Software, Methodology, Investigation, Conceptualization. **E.A.S. Marques:** Resources, Conceptualization. **M. Fabra-Rodriguez:** Writing – review & editing, Validation, Methodology. **L.F.M. da Silva:** Supervision, Conceptualization. **M. Sánchez-Lozano:** Writing – review & editing, Visualization, Formal analysis.

Declaration of competing interest

The authors declare that they have no known competing financial interests or personal relationships that could have appeared to influence the work reported in this paper.

Data availability

No data was used for the research described in the article.

References

[1] A. Elmarakbi, "Advanced Composite Materials for Automotive Applications: Structural," 2013. https://books.google.es/books/about/Advanced_Composite_Materials_for_Automot.html?id=wfxQAQAAQBAJ&redir_esc=y (accessed Jun. 11, 2024).

[2] Mangino E, Carruthers J, Pitarresi G. The future use of structural composite materials in the automotive industry. Int J Veh Des 2007;44(3–4):211–32. https://doi.org/10.1504/IJVD.2007.013640.

[3] Choi CH, Park SS, Hwang TW. Development of composite body panels for a lightweight vehicle. J Mater Manuf 2001;110. doi: www.jstor.org/stable/i40197106.

[4] Muñoz JA, Cabrera JM, Bolmaro RE, Romero Reséndiz L, Trzepiecí Nski T, Najm SM. Current trends in metallic materials for body panels and structural members used in the automotive industry. Mater Jan 2024;17(3):590. https://doi.org/10.3390/MA17030590.

[5] Leger R, Roy A, Grandidier JC. A study of the impact of humid aging on the strength of industrial adhesive joints. Int J Adhes Adhes Jul. 2013;44:66–77. https://doi.org/10.1016/J.IJADHADH.2013.02.001.

[6] Tan W, Na J, Wang G, Xu Q, Shen H. The effects of service temperature on the fatigue behavior of a polyurethane adhesive joint. Int J Adhes Adhes 2021;107. https://doi.org/10.1016/j.ijadhadh.2021.102819.

[7] Baek D. Mechanical characterization of core-shell rubber/epoxy polymers for automotive structural adhesives as a function of operating temperature. Polymers (Basel) 2021;13. https://doi.org/10.3390/polym13050734.

[8] Korta J, Mlyniec A, Uhl T. Experimental and numerical study on the effect of humidity-temperature cycling on structural multi-material adhesive joints. Compos Part B Eng 2015. https://doi.org/10.1016/j.compositesb.2015.05.020.

[9] Banea MD, da Silva LFM. Mechanical characterization of flexible adhesives. J Adhes 2009;85(4–5):261–85. https://doi.org/10.1080/00218460902881808.

[10] Machado JJM, Nunes PDP, Marques EAS, Da Silva LFM. Adhesive joints using aluminium and CFRP substrates tested at low and high temperatures under quasi-static and impact conditions for the automotive industry. Compos Part B Eng 2018. https://doi.org/10.1016/j.compositesb.2018.09.067.

[11] Viana G, Costa M, Banea MD, Da Silva LFM. A review on the temperature and moisture degradation of adhesive joints. Proc Inst Mech Eng Part L J Mater Des Appl Aug. 2017;231(5):488–501. https://doi.org/10.1177/1464420716671503.

[12] Galvez P, Abenojar J, Martinez MA. Durability of steel-CFRP structural adhesive joints with polyurethane adhesives. Compos Part B Eng 2018. https://doi.org/10.1016/j.compositesb.2018.11.097.

[13] Salimi S, Babra TS, Dines GS, Baskerville SW, Hayes W, Greenland BW. Composite polyurethane adhesives that debond-on-demand by hysteresis heating in an oscillating magnetic field. Eur Polym J 2019. https://doi.org/10.1016/j.eurpolymj.2019.109264.

[14] Ke L, Li C, He J, Dong S, Chen C, Jiao Y. Effects of elevated temperatures on mechanical behavior of epoxy adhesives and CFRP-steel hybrid joints. Compos Struct 2019. https://doi.org/10.1016/j.compstruct.2019.111789.

[15] Chiminelli A, Valero C, Lizaranzu M, López CI, Canales M. Modelling of bonded joints with flexible adhesives. J Adhes Jun. 2019;95(5–7):369–84. https://doi.org/10.1080/00218464.2018.1562347.

[16] Guedes RM, Sá A, De Moura MFSF. "Test Method An experimental and numerical assessment of DCB tests on glass/polyester curved beams cut out from pipes," Polym Test 27, 985–994, 10.1016/j.polymertesting.2008.08.011.

[17] da Silva LFM, Campilho RDSG. Advances in numerical modelling of adhesive joints. SpringerBriefs Appl Sci Technol 2012;9783642236075:1–93. https://doi.org/10.1007/978-3-642-23608-2_1/FIGURES/64.

[18] Shim W, et al. Simulating rate-and temperature-dependent behaviors of adhesives using a nonlinear viscoelastic model. Mech Mater 2020. https://doi.org/10.1016/j.mechmat.2020.103446.

[19] Hesebeck O, Wulf A. Hyperelastic constitutive modeling with exponential decay and application to a viscoelastic adhesive. Int J Solids Struct Jun. 2018;141–142:60–72. https://doi.org/10.1016/J.IJSOLSTR.2018.02.011.

[20] Holzapfel GA. Nonlinear solid mechanics : a continuum approach for engineering. Wiley 2000:455.

[21] Kim B, et al. A comparison among neo-hookean model, mooney-rivlin model, and ogden model for chloroprene rubber. Int J Precis Eng Manuf May 2012;13(5):759–64. https://doi.org/10.1007/s12541-012-0099-y.

[22] Ali. A review of constitutive models for rubber-like materials. Am J Eng Appl Sci 2010;3(1):232–9. https://doi.org/10.3844/ajeassp.2010.232.239.

[23] Simón-Portillo FJ, Abellán-López D, Arán F, Da Silva LFM, Sánchez-Lozano M. Methodology for the mechanical characterisation of hyperelastic adhesives. experimental validation on joints of different thicknesses. Polym Test 2023;129:108286. https://doi.org/10.1016/j.polymertesting.2023.108286.

[24] Graf A. Aluminum alloys for lightweight automotive structures. Mater Des Manuf Light Veh Jan. 2021:97–123. https://doi.org/10.1016/B978-0-12-818712-8.00003-3.

[25] Cognard P, "Adhesives and sealants : basic concepts and high tech bonding," p. 492, 2005.

[26] Roig A, Molina L, Serra A, Santiago D, De la Flor S. Structural reversible adhesives based on thiol-epoxy vitrimers. Polym Test 2023;128:108205. https://doi.org/10.1016/j.polymertesting.2023.108205.

[27] Anderson BJ. Thermal stability of high temperature epoxy adhesives by thermogravimetric and adhesive strength measurements. Polym Degrad Stab 2011. https://doi.org/10.1016/j.polymdegradstab.2011.07.010.

[28] Tan W, Jingxin N, Guangbin W, Chen H, Meng H. Effect of temperature on the fatigue performance and failure mechanism of a flexible adhesive butt joint. J Adhes 2022;98(13):1998–2028. https://doi.org/10.1080/00218464.2021.1950537.

[29] Tan W, Na J, Wang G, Xu Q, Shen H, Mu W. The effects of service temperature on the fatigue behavior of a polyurethane adhesive joint. Int J Adhes Adhes 2021;107:102819. https://doi.org/10.1016/j.ijadhadh.2021.102819.

[30] Crocker LE, Duncan BC, Hughes RG, Urquhart JM, "Hyperelastic Modelling of Flexible Adhesives," no. May, pp. 1–42, 1999.

[31] Moreira DC, Nunes LCS. Comparison of simple and pure shear for an incompressible isotropic hyperelastic material under large deformation. Polym Test Apr. 2013;32(2):240–8. https://doi.org/10.1016/J.POLYMERTESTING.2012.11.005.

[32] Xia Y, Dong Y, Xia Y, Li W. A novel planar tension test of rubber for evaluating the prediction ability of the modified eight-chain model under moderate finite deformation. Rubber Chem Technol 2005;78(5):879–92. https://doi.org/10.5254/1.3547920.

[33] Schreier H, Orteu JJ, Sutton MA. Image correlation for shape, motion and deformation measurements: Basic concepts, theory and applications. Image Correl Shape, Motion Deform Meas Basic Concepts, Theory Appl 2009:1–321. https://doi.org/10.1007/978-0-387-78747-3.

[34] M. Z. Siddiqui, F. Tariq, and N. Naz, "Application of a two step digital image correlation algorithm in determining poisson's ratio of metals and composites," in *62nd International Astronautical Congress 2011, IAC 2011*, 2011, vol. 7, pp. 6062–6069.

[35] "Tracker Video Analysis and Modeling Tool for Physics Education." https://physlets.org/tracker/ (accessed Jul. 26, 2023).

[36] Dorfmann A, Fuller KNG, Ogden RW. Shear, compressive and dilatational response of rubberlike solids subject to cavitation damage. Int J Solids Struct Apr. 2002;39(7):1845–61. https://doi.org/10.1016/S0020-7683(02)00008-2.

[37] Lou W, Xie C, Guan X. Thermal-aging constitutive model for a silicone rubber foam under compression. Polym Degrad Stab 2022;198:109873. https://doi.org/10.1016/j.polymdegradstab.2022.109873.

[38] Gehre C, Gades H, Wernicke P, "Objective rating of signals using test and simulation responses," in *Processding of 21st International Technical Conference on the Enhanced Safety of Vehicles Conference (ESV)*, 2009, pp. 15–18.